Physical modeling of slope failure during slope cutting work

Modélisation physique de rupture de talus pendant des travaux de déblais de talus

K. Itoh, S. Timpong & Y. Toyosawa
National Institute of Occupational Safety and Health, Tokyo, Japan
S. B. Tamrakar
C-way engineering, Hokkaido, Japan
N. Suemasa
Musashi Institute of Technology, Tokyo, Japan

ABSTRACT

Full-scale slope model tests and centrifuge model tests were conducted to examine the mechanism of slope failure during slope cutting works. It was found that local slope failure was observed before complete slope failure and this mechanism was consistent with previous slope failure accidents. The horizontal and vertical movements of the slope could be measured during excavation, so it may be possible to predict slope failure from the typical slope movement in order to prevent slope failure accidents in future.

RÉSUMÉ

Des tests sur modèles de talus grandeur nature et des tests sur modèles centrifuges ont été effectués pour examiner le mécanisme de rupture de talus pendant les travaux de déblais de talus. Il s'est avéré qu'une rupture de talus localisée était observée avant la rupture de talus totale et que ce mécanisme était cohérent avec les accidents de rupture de talus antérieurs. Les mouvements horizontal et vertical du talus ont pu être mesurés pendant l'excavation; il semble ainsi possible de prédire une rupture de talus à partir d'un glissement de terrain typique pour éviter un accident de rupture de talus dans l'avenir.

Keywords: Centrifuge model test, field test, slope cutting, slope failure

1 INTRODUCTION

In general, excavated slopes appear to be stable when they are either excavated to a safe slope angle or when effective protective measures are taken. The slopes are at greater risk of failure during slope cutting works, and slope failures have often occurred suddenly without any clear signs of failure, giving construction workers no time to avoid accidents. In Japan, there are approximately 30 to 40 slope failure accidents every year, causing injury and death to workers and damage to property. According to labor accident reports from the Japan Construction Safety and Health Association, more than 50% of these accidents occurred while excavating or leveling the lower parts of the slope toe as shown in Fig. 1. Therefore, it is necessary to develop an early warning system to prevent such accidents during slope cutting works.

Figure 1 Typical example of labor accident during slope cutting works

Although many instruments for monitoring landslides have been developed to measure the movement of the slope just before failure, most of them are either difficult to set up at the construction site or are too expensive to use for small- to medium-scale slope cutting projects. In this paper, a simple and cost-effective slope monitoring system for a small- to medium-scale slope cutting site was developed, and the mechanism of slope failure was investigated by conducting full-scale slope model tests in the field and small-scale slope model tests using the centrifuge modeling technique.

2 FIELD TEST

2.1 *Field test setup*

In the field tests, full-scale model slopes were prepared by placing Narita sand on natural ground (Kanto loam), where the average height of each filled layer was about 0.5 m with the inclination of about 1:1.5 (33°). In case of the model slope with loose ground condition (Case-F1), additional compaction was not applied to each filled layer. However, for the model slope with dense ground condition (Case-F2), each filled layer was compacted by five passes of a small bulldozer (7-ton, with a bearing pressure of 25.5kPa). The final shape of the full-scale model slope was trimmed by a backhoe, in which the height, width and slope angle of each model slope were 5m, 3.5m and 45 degrees, respectively. Figure 2 shows the typical setup of the model slope in the field. In-situ tests were also conducted on the slope to determine the physical properties. Table 1 shows the physical properties of the model slope.

Proceedings of the 17th International Conference on Soil Mechanics and Geotechnical Engineering
M. Hamza et al. (Eds.)

doi:10.3233/978-1-60750-031-5-522

Figure 2 Field test setup

Table 1 Physical properties of the model slope

Case	F1	F2
Material	Narita sand	
Number of rolling passes	0	5
Water content w (%)	29.4	27.43
Wet density ρ_t (g/cm^3)	1.67	1.74
Dry density ρ_d (g/cm^3)	1.29	1.37

2.2 *Test procedure*

The model slope was excavated in steps, vertically from the slope face downward to the slope toe using the backhoe. The width and height of each excavation were 2.5m and 0.5m, respectively. After each excavation, the slope was left for about 5 minutes to evaluate the signs of slope failure. The slope cutting was continued until the slope failed completely. In order to monitor the slope movement during the excavation, an invar wire extensometer and optical two-dimensional (2D, x-y directions) displacement sensor were installed on the top of the slope as presented in Fig. 3.

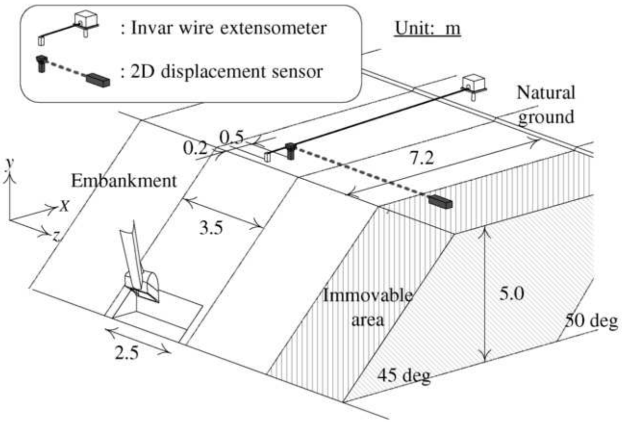

Figure 3 Schematic view of the field test setup

2.3 *Field test results*

Figure 4 shows the slope movement with elapsed time measured by the invar wire extensometer and the 2D displacement sensor for the model slope Case-F1 (loose ground). The excavated heights and slope failure events are also indicated in the same figure. Figure 5 shows photographs of the typical slope failure. During the 5th excavation (excavated height of 2.5m), slope movement of about 2mm was detected by the invar wire extensometer and 2D displacement sensor (y-direction), and a local slope failure occurred immediately after the last scoop at the 5th excavation (Fig. 5(a)). Thereafter, gradual movement of the slope was observed by the 2D displacement sensor (x-direction). During the 6th excavation (excavated height of 3.0m), rapid movement was observed in all sensors just before the second slope failure (Fig. 5(b)). The excavation was stopped to observe the collapsed shape, and during this observation the third collapse of the slope occurred as shown in Fig. 5(c).

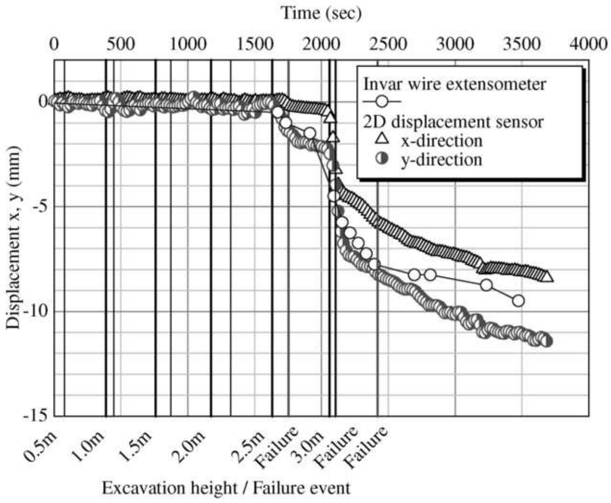

Figure 4 Slope movements in the model slope Case-F1

(a) The 1st failure (b) The 2nd failure (c) The 3rd failure

Figure 5 Slope failure events in the model slope Case-F1

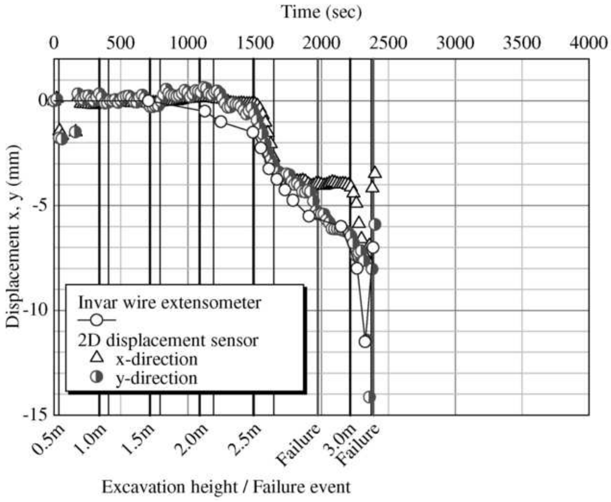

Figure 6 Slope movements in the model slope Case-F2

(a) the 1st failure (b) the 2nd failure

Figure 7 Slope failure events in the model slope Case-F2

As shown in Fig. 6, in case of model slope Case-F2 (dense ground), about 3mm of slope displacement was observed at all sensors during the 5th excavation (excavated height of 2.5m). After the excavation, the slope deformation continued to increase and local slope failure was observed as seen in Fig. 7(a). Finally, a large-scale collapse from the slope crest occurred immediately after the 6th excavation was conducted, as seen in Fig. 7(b).

3 CENTRIFUGE MODEL TEST

Centrifuge model tests were conducted to examine the failure mechanism of the full-scale slopes, under equivalent conditions to the full-scale slope model test. All the tests described here were conducted using the JNIOSH NIIS Mark II Centrifuge (Horii et al., 2006).

3.1 *Centrifuge model test setup*

An aluminum model box with internal dimensions of 200mm wide, 450mm long and 270mm high was used. A perspex window was installed on the front of the box for visually observing the model during the centrifuge test. Narita sand taken from the collapsed part in the field test was used for preparing the model slope. The natural grain size of the sand was adjusted to a maximum of 2mm to minimize the scale effect in the centrifuge test. The sand was placed in the model box and compacted by a Bellofram cylinder. The compaction pressure was controlled to achieve the similar ground density as presented in the field test. Table 2 shows the conditions of the centrifuge model test. The geometry of the model slope was set to correspond to 1/25 scale of the full-scale model slope in the field test. Figure 8 shows a schematic view of the experimental model and arrangement of linear variable displacement transducers (LVDT). The centrifuge tests were conducted at the acceleration of 25g (25 times earth's gravity), where the model slope represented a 5m high slope with a slope angle of 45 degrees corresponding to the prototype scale. At the acceleration of 25g, an in-flight excavator (Toyosawa et al., 1998) was used for simulating slope cutting in the centrifuge. The movement of the in-flight excavator was controlled manually from the computer room. The model slope was excavated in steps up to the occurrence of slope failure, where the excavated height of each step was about 20mm (0.5m in prototype scale). The excavation step was executed at 2-minute intervals. After complete slope failure was observed, the centrifuge test was terminated.

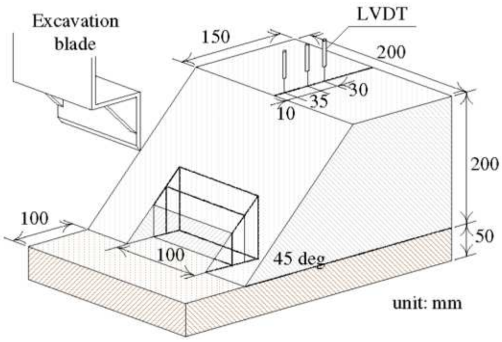

Figure 8 Schematic view of the centrifuge model test setup

Table 2 Centrifuge model test conditions

Case	C1	C2
Material	Narita sand	
Water content w (%)	22.9	21.1
Wet density ρ_t (g/cm³)	1.694	1.790
Simulated field test case	F1	F2

3.2 *Centrifuge model test results*

For the model slope Case-C1 (loose ground), the slope movement measured by the displacement transducer (LVDT) with elapsed time from attainment of 25g is presented in Fig. 9 and typical photographs of slope failures are shown in Fig. 10. As the settlement at the top of the slope largely increased immediately after the applied acceleration reached 25g, the excavation was started when the increase in settlement became relatively small. During the excavation, the displacement gradually increased especially near the slope face, and local collapse in the slope was observed immediately after the 3rd excavation (excavated height of 1.5m) as shown in Fig. 10(a). The second local slope failure occurred at about 45 seconds after the 4th excavation (excavated height of 2.0m) as seen in Fig. 10(b) and complete slope failure was observed when the excavated height became 3.0m as shown in Fig. 10(c). Comparing the excavated height (1.5m) at the first collapse observed in the centrifuge test with that in the field test (2.5m), the excavated height at failure was quite different. However, the shape of the slope failure observed in the centrifuge test was similar to that in the field test.

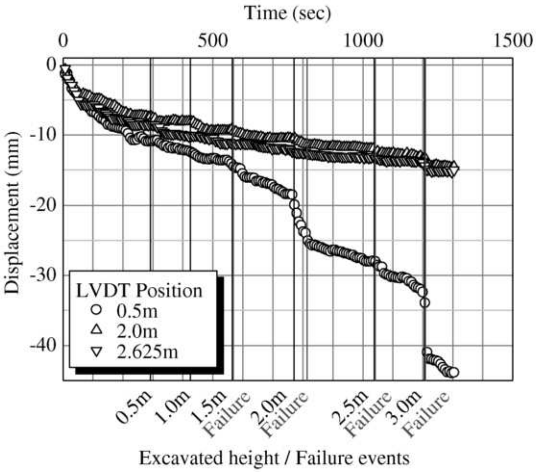

Figure 9 Slope movements in the model slope Case-C1

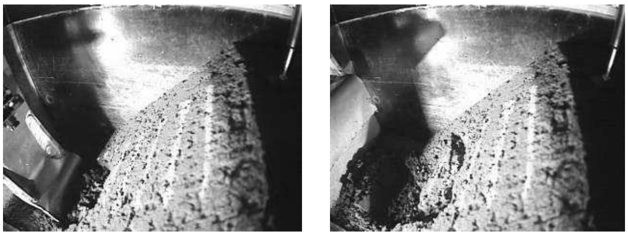

(a) 1st local failure (b) 2nd local failure

(c) complete slope failure

Figure 10 Slope failure events in the model slope Case-C1

Figure 11 shows the slope movement with elapsed time for the model slope Case-C2 (dense ground). The displacement gradually increased with the increase of excavated height. It should be noted that a larger increment of displacement was observed at the displacement sensor located near the slope face (0.5m) than those at the other sensors. At the 1st excavation (excavated height of 0.5m), large displacement was observed at the sensor located near the slope face. It appears that the large displacement was caused by the bedding error of the displacement transducer. The local collapse in the slope occurred immediately after the 5th excavation (excavated height of 2.5m) as shown in Fig. 12. Figure 13 directly compares the measured displacement caused by each step of slope cutting between the field test and the centrifuge model test. In case of model slopes Case-F1 and Case-C1 (loose ground condition), when the excavated height was less than 2m, large displacement was only observed in the centrifuge test and the displacement observed at the collapsing excavation stage in the centrifuge test was about 1.5 times that observed in the field test. This is probably attributed to the difference in the condition of slope failure observed in both tests. On the other hand, in case of model slopes Case-F2 and Case-C2 (dense ground condition), the deformation behavior and condition of slope failure agreed well between the centrifuge model test and the field test as seen in the figure. The difference of the collapse condition and deformation behavior observed in the centrifuge model test and full-scale slope model test in the field test was probably due to many factors, such as the difference in compaction density, water content, boundary condition in both tests and the scale effect of the soil particle size presented in the centrifuge model test. Further research considering all of these factors may be needed in order to attain a better simulation of the field test using the centrifuge modeling technique.

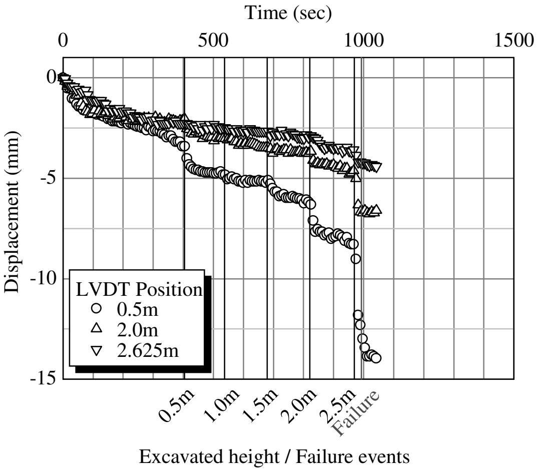

Figure 11 Slope movements in the model slope Case-C2

Figure 12 Slope failure event in the model slope Case-C2

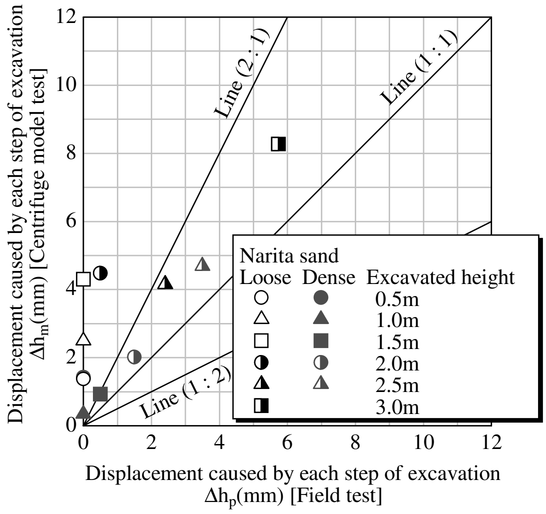

Figure 13 Direct comparison of the measured displacement caused by each step of slope cutting in the field test and centrifuge model test

4 CONCLUSION

The full-scale slope model test and the small-scale centrifuge model test were conducted to examine the mechanism of slope failure caused by slope cutting works. The main conclusions are as follows:

1. Based on the field test results it was found that in all cases local failure of the excavated slope occurred before complete slope failure. This mechanism is consistent with previous slope failure accidents that occurred during slope cutting works.
2. The horizontal and vertical movements of the slope could be measured during the field test, so it is possible to predict the movement of the slope before failure and to prevent labor accidents caused by slope failure in future.
3. Reasonably good agreement in the conditions and shape of slope failure was found between the field test and the centrifuge model test.

ACKNOWLEDGEMENT

The authors are grateful to Mr. Tetsuya Kondo and Mr. Sho Shigemura of Tokyu Construction Co., Ltd., and to Mr. Kazuyuki Nakamura and Mr. Hideo Hashizume of Geodesign Co., Ltd. who collaborated on constructing the full-scale model slope for the field test. The authors also would like to thank Ms. Sumine Kusakabe and Mr. Takuma Koitabashi. former students of Musashi Institute of Technology, for making a model slope in the centrifuge model test.

REFERENCES

Horii, N., Itoh, K., Toyosawa, Y. and Tamate, S. 2006. Development of the NIIS Mark-II geotechnical centrifuge, the 6th International Conference on Physical Modelling in Geotechnics, Ng, Zhang and Wang (eds.), Taylor & Francis, pp. 141-146.

Japan Construction Safety and Health Association. 1989-2004. Construction industrial labor accident reports. Construction Safety and Health Yearbooks.

Toyosawa, Y., Horii, N., Tamate, S., Suemasa, N. and Katada, T. 1998. Failure mechanism of anchored retaining wall, Proceedings of International Conference on Centrifuge Modelling-Centrifuge 98, Tokyo, Kimura, Kusakabe, and Takemura (eds), Balkema, Rotterdam, pp. 667-672.